

Title	Oxalate efflux transporter from the brown rot fungus <i>Fomitopsis palustris</i> .
Author(s)	Watanabe, Tomoki; Shitan, Nobukazu; Suzuki, Shiro; Umezawa, Toshiaki; Shimada, Mikio; Yazaki, Kazufumi; Hattori, Takefumi
Citation	Applied and environmental microbiology (2010), 76(23): 7683-7690
Issue Date	2010-12
URL	http://hdl.handle.net/2433/134573
Right	© 2010, American Society for Microbiology
Type	Journal Article
Textversion	author

1
2 Title: An oxalate efflux transporter from the brown-rot fungus *Fomitopsis palustris*

3 Running title: Oxalate transporter from *Fomitopsis palustris*

4 Tomoki Watanabe¹, Nobukazu Shitan^{1,3}, Shiro Suzuki², Toshiaki Umezawa^{1,2}, Mikio
5 Shimada^{1,4}, Kazufumi Yazaki¹, and Takefumi Hattori^{1*}

6 ¹*Research Institute for Sustainable Humanosphere, Kyoto University, Uji, Kyoto 611-0011,*
7 *Japan;*

8 ²*Institute of Sustainable Science, Kyoto University, Uji, Kyoto 611-0011, Japan;*

9 ³*Present address: Laboratory of Natural Medicinal Chemistry, Kobe Pharmaceutical*
10 *University, 4-19-1 Motoyamakita-machi, Higashinada-ku, Kobe 658-8558, Japan;*

11 ⁴*Present address: Environmental and Biotechnological Frontier Engineering, Fukui*
12 *University of Technology, Fukui 910-8505, Japan*

13 *Address correspondence to: Takefumi Hattori, Research Institute for Sustainable
14 Humanosphere, Kyoto University, Uji, Kyoto 611-0011, Phone: +81 774 38 3626. Fax: +81
15 774 38 3682. E-mail address: thattori@rsh.kyoto-u.ac.jp

16
17 Journal Section: Mycology
18

Abstract

An oxalate-fermenting brown-rot fungus, *Fomitopsis palustris*, secretes large amounts of oxalic acid during wood decay. Secretion of oxalic acid is indispensable for the degradation of wood cell walls, but almost nothing is known about the transport mechanism by which oxalic acid is secreted from *F. palustris* hyphal cells. We characterized the mechanism for oxalate transport using membrane vesicles of *F. palustris*. Oxalate transport in *F. palustris* was ATP dependent and was strongly inhibited by several inhibitors such as valinomycin and NH_4^+ , suggesting the presence of a secondary oxalate transporter in this fungus. We then isolated a cDNA, *Fomitopsis palustris* Oxalic Acid Resistance (*FpOAR*), from *F. palustris* by functional screening of yeast transformants with cDNAs grown on oxalic acid-containing plates. *FpOAR* is predicted to be a membrane protein that possesses six transmembrane domains, but shows no similarity with known oxalate transporters. The yeast transformant possessing *FpOAR* (*FpOAR*-transformant) acquired resistance to oxalic acid and contained less oxalate than the control transformant. Biochemical analyses using membrane vesicles of the *FpOAR*-transformant showed that the oxalate transport property of *FpOAR* was consistent with that observed in membrane vesicles of *F. palustris*. The quantity of *FpOAR* transcripts was correlated with increasing oxalic acid accumulation in the culture medium and was induced when exogenous oxalate was added to the medium. These results strongly suggest that *FpOAR* plays an important role in wood decay by acting as a secondary transporter responsible for secretion of oxalate by *F. palustris*.

Oxalic acid is produced by a wide variety of members of five kingdoms (*Monera*, *Protista*, *Fungi*, *Plantae*, and *Animalia*) (32), and plays multiple roles as a proton and electron source and strong metal chelator in ecosystem processes (11). With regard to wood decay by brown-rot fungi, which cause severe damage to wooden structures, oxalic acid is secreted by the fungus in large amounts (8, 38). Several important roles of oxalic acid in the brown-rot decay process are proposed. Oxalic acid hydrolyzes side-chains of hemicelluloses, then depolymerizes the hemicellulose backbones and amorphous cellulose, thus increasing the porosity of the wood structure to the hyphal sheath, decay enzymes, or other low-molecular-weight decay agents (12). In cellulose degradation by the Fenton reaction, a low concentration of oxalate promotes degradation (41) by facilitating hydroxyl radical formation (45), but a higher concentration of the acid inhibits the degradation (41) and radical formation (45). Furthermore, oxalate forms Fe-oxalate complexes, which can then diffuse into the wood cell wall for the Fenton reaction by which oxalate protects the hyphae of brown-rot fungi from attack by the Fenton reagent (2, 16, 38). Therefore, from the viewpoint of preservation of wooden buildings and cultural treasures, elucidation of the biochemical mechanisms for oxalate biosynthesis and its secretion in brown-rot fungi is needed.

Recently, we clarified the mechanisms for oxalate biosynthesis in the brown-rot basidiomycete *Fomitopsis palustris*, which is used as a standard fungus for Japanese Industrial Standards decay resistance tests. *Fomitopsis palustris* secretes large amounts of oxalate (33–78 mM) into the culture fluid, which lowers the medium pH to ca. 2. The terminal enzymes for oxalate biosynthesis are cytosolic oxaloacetate acetylhydrolase

(OAAH, EC 3.7.1.1) (1) and peroxisomal cytochrome *c* dependent glyoxylate dehydrogenase (15, 43). Our biochemical analysis of oxalate fermentation by *F. palustris* led to the conclusion that the fungus acquires energy for growth by oxidizing glucose mainly to oxalate through the tricarboxylic acid (TCA) and glyoxylate (GLOX) cycles (28, 29, 35).

Importantly, it is widely recognized that oxalate is toxic to organisms. Exogenously added oxalate inhibits sporulation and growth of the filamentous fungi *Fusarium oxysporum* (7) and *Pythium vexans* (46). Therefore, oxalate-producing brown-rot fungi must have a mechanism to prevent damage caused by intra- and extra-cellular oxalate. Several brown-rot fungi show not only oxalate-producing but also oxalate-degrading activity. Among these oxalate-producing and -degrading brown-rot fungi, *Postia placenta* produces oxalate decarboxylase to convert oxalate to formate and CO₂ (25), which prevents overaccumulation of oxalic acid and forms a non-toxic, buffered, low-pH environment that facilitates the brown-rot decay process (26). *Gloeophyllum trabeum* degrades extracellularly added oxalate to give rise to CO₂ (10). Similarly, *Fomitopsis pinicola* and *Meruliporia incrassata* have been reported to decrease the amount of extracellular oxalate (36).

In contrast to these oxalate-producing and -degrading brown-rot fungi, oxalate-decomposing activity has not been reported for *F. palustris*. However, *F. palustris* grows vigorously in the presence of a high oxalate concentration (28, 29). The marked accumulation of oxalic acid in the culture fluid of *F. palustris* suggests that the fungus has an efficient system to transport oxalate out of the cells. Oxalate is continuously biosynthesized as a major end product of primary metabolism in the cytosol and

84 peroxisome of *F. palustris* (15, 28, 35). Thus, while transporting oxalate from the
85 peroxisome to the cytosol and eventually out of the cells, essential metabolic processes
86 should be protected from oxalate toxicity. In this context, the oxalate transporter in the
87 cytosolic membrane is expected to reduce the intracellular concentration of oxalate, which
88 probably contributes to the oxalate resistance system in *F. palustris*. However, almost
89 nothing is known about the transport systems of *F. palustris*.

90 Oxalate transporters are known to play several important roles in metabolizing or
91 excreting oxalate by other organisms. For example, *Oxalobacter formigenes*, a
92 gram-negative anaerobe, possesses the oxalate:formate exchange protein OxIT, which is
93 essential for *O. formigenes* to produce ATP (21). Humans and mice possess the SLC26
94 multifunctional anion exchangers, of which SLC26A6 (humans) and Slc26a6 (mice) are
95 proposed to exchange Cl^- and SO_4^{2-} for oxalate or formate in the intestinal villi, renal
96 proximal tubule and cardiac myocytes (27). Furthermore, hepatopancreatic lysosomal
97 membrane vesicles isolated from the lobster *Homarus americanus* exchange oxalate for Cl^-
98 in relation to Zn^{2+} detoxification (40).

99 Recently, Mch5, a homolog of a putative oxalate:formate antiporter from *Aspergillus*
100 *fumigatus*, was postulated to be a putative oxalate transporter in yeast *Saccharomyces*
101 *cerevisiae*. However, the oxalate-transporting activity of Mch5 and the possible roles of the
102 gene product have not been demonstrated (5). Accordingly, an oxalate-transporting protein
103 has not previously been characterized experimentally from any fungus.

104 Here we describe a cDNA encoding the protein involved in oxalate transport in *F.*
105 *palustris*. To isolate a cDNA encoding the oxalate transporter, we previously isolated

106 fungal cDNAs from yeast transformants with cDNA of *F. palustris* grown in the presence
107 of a high oxalate concentration that is lethal to wild-type cells (49). Even if oxalate was
108 incorporated into the cells, the transformants probably transported oxalate out of the cells or
109 it was degraded by the gene products of the cDNA from *F. palustris*. Accordingly, these
110 cDNAs were expected to encode transporters catalyzing oxalate transport out of the cells or
111 oxalate-decomposing enzymes and other proteins possessing unidentified functions. By this
112 strategy, we successfully isolated the cDNA *FpTRP26* conferring oxalic acid resistance for
113 *F. palustris* (49). We have further characterized the remaining transformants showing oxalic
114 acid resistance (49) and obtained the gene product, FpOAR (*Fomitopsis palustris* Oxalic
115 Acid Resistance), which is a putative plasma membrane protein that showed distinct
116 oxalate transport activity in yeast membrane vesicles. The oxalate transport property of
117 FpOAR was similar to that of *F. palustris* membrane vesicles. These results strongly
118 suggest that FpOAR is involved in oxalate secretion in *F. palustris* hyphal cells.

119 120 MATERIALS AND METHODS

121
122 ***Fomitopsis palustris* culture conditions.** Two mycelial plugs (5 mm in diameter) of *F.*
123 *palustris* (Berkely et Curtis) Murill TYP6137 were grown as a stationary culture in a 200
124 ml Erlenmeyer flask containing 40 ml liquid medium as previously reported (49).

125 **Cloning of *F. palustris* cDNA conferring oxalic acid resistance.** Functional screening
126 of a *Saccharomyces cerevisiae* AD12345678 (6) transformant with a *F. palustris* cDNA
127 library with vector pDR196 (51) was carried out to screen the transformants to grow with

12 mM oxalic acid (49). Because the cDNA fragment recovered from oxalic acid-resistant yeast showing a strong phenotype lacked the 5' region, the 5' end of the cDNA was determined with the Gene Racer™ kit (Invitrogen) according to the manufacturer's instructions. The 5' end of the cDNA was cloned with the gene-specific antisense PCR primer 5'-CCACGACCACCGCCGCAAGCATGAAGA-3'. The amplified cDNA fragments were subcloned into the TA cloning vector with the pCR2 TOPO TA cloning kit (Invitrogen). A clone containing an insert of the expected size was sequenced. The open reading frame (ORF) of the cDNA was cloned with the PCR primers 5'-ACTAGTATGACCGACCTGCATCGAAG-3' (sense) and 5'-GGATCCTCAGAGAAGATCTTCTTGCCG-3' (antisense), which were gene-specific primers containing *Spe* I and the *Bam*HI restriction site, respectively. The coding region thus obtained was named *FpOAR* (*Fomitopsis palustris* Oxalic Acid Resistance).

Characterization of oxalic acid-resistance activity of FpOAR. The plasmid containing *FpOAR* was reintroduced into the *S. cerevisiae* AD12345678 strain to characterize its oxalic acid resistance according to our method reported previously (49). Oxalic acid resistance was determined by growth of the yeast transformant. Similarly, the transformants were cultivated separately on SD (–Ura) plates containing different HCl concentrations (pH 1.5, 1.6, and 2.2).

Quantification of oxalic acid. Oxalic acid in the *F. palustris* culture medium was quantified with a commercial kit after the pH of the medium was adjusted for the assay (Roche, Germany) (48), while GC-MS analysis (14) was conducted for that in yeast cells. Yeast (OD₆₀₀ 0.1) was cultured at 30°C in 50 ml SD (–Ura) liquid medium containing 2

mM oxalic acid until OD₆₀₀ 1.0–2.0. The cells were harvested by centrifugation at 1000×g for 10 min and washed twice with cold distilled water. The dry weight of cells was determined after freeze-drying for 5 h. To the dried cells, 250 µl 1N HCl and 600 µl ethylacetate were added and cells were homogenized with glass beads (Toshinriko, No. 04) for 4 min. The oxalic acid extracted with ethylacetate was quantified as previously described (14).

GC-MS (EI) was performed on a Shimadzu GC-MS QP-5050A. The column conditions were as follows: CBP1-M25-025, 25 m × 0.22 mm (i.d.) (Shimadzu), column temperature 80–240°C (8°C/min), carrier gas He, and carrier gas flow rate 0.8 ml/min.

Quantitative real-time PCR analysis of gene transcription. Total RNA was isolated from *F. palustris* mycelia with the RNeasy Plant Mini Kit (Qiagen). First-strand cDNA synthesis was performed with Superscript II reverse transcriptase (Invitrogen) using 0.2 µg RNA. Real-time quantitative PCR was performed with a 7300 Real Time System (Applied Biosystems) and amplicons were detected with SYBR Green (Applied Biosystems). Quantifications of the amplicons were based on standard curves prepared for each target cDNA. The gene-specific primers 5'-CCTCGAACAAGCGAATTCTCTTT-3' and 5'-AGTGTCCCGCCGAGGAA-3' were used to generate an 85 bp amplicon for *FpOAR* transcripts. The amount of transcripts was normalized by comparison with those of a 75 bp amplicon derived from either total RNA or 28S rRNA (GenBank accession no. AY515333) with the primers 5'-TGACACGGACTACCAGTGCTTT-3' (sense) and 5'-CACCCATTTTGAGCTGCATTC-3' (antisense).

FpOAR transcripts were quantified in mycelia from cultures to which either oxalate (50 mM final concentration) or H₂O was added on day 3. The cultures were incubated for 12 h prior to RNA extraction.

Preparation of *F. palustris* membrane vesicles. The membrane vesicles were prepared from *F. palustris* hyphal cells as described previously (33). Cells were collected and homogenized in ice-cold homogenizing buffer (0.1 M Tris-HCl, pH 8.0, 10% [v/v] glycerol, 5 mM EDTA; 2 ml/g fresh weight of mycelia) using a Phoenix blender (USA). Prior to use, KCl, DTT, and PMSF were added to the autoclaved buffer at the final concentrations 150 mM, 3.3 mM and 1 mM, respectively, and the mixture was stirred for 1 min. Unbroken cells and debris were removed by centrifugation twice at 8,000×g for 10 min. The supernatants were pooled and centrifuged at 100,000×g for 60 min. The microsome fraction was resuspended with autoclaved resuspension buffer (10 mM Tris-HCl, pH 7.6, 10% [v/v] glycerol, 1 mM EDTA). Isolated membrane vesicles were stored at –80°C in resuspension buffer containing 1 mM DTT and 1 mM PMSF until use.

Yeast membrane vesicles for *in vitro* transport studies were isolated as described previously (17, 44) with the following modifications. The *S. cerevisiae* AD12345678 strain was grown overnight in SD (–Ura) liquid medium to OD₆₀₀ 1–2. Cells were washed twice with water and resuspended to OD₆₀₀ 1–2 in spheroplast buffer (1.1 M sorbitol, 20 mM Tris-HCl [pH 7.6], 1 mM DTT containing 57 units/ml Zymolyase 20T). After cell wall digestion was completed, spheroplasts were collected by centrifugation at 1200×g for 10 min. Cell lysis was performed gently on ice in 25 ml breaking buffer (1.1 M glycerol, 50 mM Tris-ascorbate [pH 7.4], 5 mM EDTA, 1 mM DTT, 1.5% polyvinylpyrrolidone, 2

mg/ml BSA, 1 mM PMSF, 10 µg/ml leupeptin, 2 µg/ml aprotinin, and 2 µg/ml pepstatin) with a Dounce homogenizer and 40 strokes with a tight-fitting glass piston. Unbroken cells and debris were removed by centrifugation twice at 3,000×g for 10 min. The supernatants were pooled and centrifuged at 100,000×g for 60 min. Microsomal membrane proteins were quantified by Bradford's method (3). The pellet was suspended to a protein concentration of about 5 mg/ml in vesicle buffer (1.1 M glycerol, 50 mM Tris-MES [pH 7.4], 1 mM EDTA, 1 mM DTT, 2 mg/ml BSA, 1 mM PMSF, 1 µg/ml leupeptin, 2 µg/ml aprotinin, and 2 µg/ml pepstatin). Small aliquots were immediately used for transport assays or stored at –80°C until use. Membrane vesicles prepared with this method are a mixture of inside-out and right-side-out orientation, whereas only inside-out vesicles can hydrolyze ATP owing to the outside orientation of the ATPase catalytic sites that drive membrane transport and because ATP cannot permeate the membrane. Therefore, in this experiment the observation of oxalate uptake into the inside-out vesicle indicates oxalate efflux activity of the hyphal cell membrane.

***In vitro* oxalate transport assay.** Vesicles (100 µg protein) were mixed with transport buffer (0.4 M glycerol, 100 mM KCl, 20 mM Tris-MES [pH 7.4], 1 mM DTT) and incubated with 0.2 mM [¹⁴C]oxalic acid at 25 °C for 10 min in the absence or presence of 5 mM MgATP with a final volume of 125 µl, unless stated otherwise. In the assay using *F. palustris* vesicles, the vesicles (500 µg protein) were suspended in a final volume of 500 µl. Uptake of [¹⁴C]oxalic acid (185 MBq/mmol) into membrane vesicles was measured by two methods. For *F. palustris* membrane vesicles, 130 µL reaction mixture was loaded on a Sephadex (G-50 fine) spin column and centrifuged at 2,000 rpm for 2 min. The

radioactivity of 100 μ L filtrate was determined with a liquid scintillation counter. The yeast vesicles were absorbed onto nitrocellulose filters (3 cm in diameter, 0.45 μ m pore size; GE Healthcare) by filtration with an aspirator. The vesicles on the membrane were washed three times with 1 ml transport buffer by filtration with an aspirator, dried on filter paper and subjected to liquid scintillation counting. Counts were corrected for background and quenching. Quantification and calculations were performed using a Liquid Scintillation Analyzer Tri-Carb 2800TR (Perkin Elmer, USA).

Effects of inhibitors on oxalate transport. Using *F. palustris* vesicles, the following inhibitors were added separately to assay solutions: 1 mM vanadate, 2 μ M valinomycin, 1 mM NH_4Cl , 150 μ M glibenclamide, or 5 μ M cyclosporin A. Oxalate transport was recorded as described above.

To assess the inhibition using yeast vesicles from the *FpOAR*-transformant, we used 5 μ M verapamil, and 5 μ M gramicidin D in addition to the reagents used for the *F. palustris* vesicle assay. Oxalate transport was recorded as described above.

Statistical analysis. Analyses were carried out using ANOVA followed by the Dunnett test with a level of significance of $p = 0.05$.

RESULTS

Biochemical analysis of oxalate transport using *F. palustris* membrane vesicles. To characterize oxalate transport of *F. palustris* we prepared membrane vesicles from hyphae of the fungus and investigated whether MgATP is required for the transport activity. In the

237 presence of MgATP, [^{14}C]oxalate uptake into the vesicles was 4.27 times that in the control
238 lacking MgATP (Fig. 1). This result indicated that MgATP is needed for oxalate transport
239 activity in *F. palustris*.

240 We then investigated the effects of a variety of inhibitors on oxalate transport. Vanadate,
241 which is an inhibitor of P-type ATPases and ATP-binding cassette (ABC) transporters,
242 reduced oxalate uptake into the membrane vesicle by 68.0%. The addition of valinomycin
243 or NH_4Cl , which abolish the $\Delta\Psi$ and ΔpH across the membrane, respectively, inhibited
244 oxalate uptake by 86.3% and 90.1%, respectively. In contrast, glybenclamide and
245 cyclosporin A, which are typical inhibitors of ABC transporters, did not influence oxalate
246 transport. These results indicate that ABC transporters are not primarily responsible for
247 oxalate transport. Collectively, the results strongly suggest that a secondary oxalate
248 transporter functions in *F. palustris*, in which $\Delta\Psi$ and ΔpH are involved.

249 **Cloning of a cDNA conferring oxalic acid resistance on the yeast transformant.**

250 Previously, we isolated the cDNA FpTRP26 from one of eight *S. cerevisiae* transformants
251 (49). From the remaining transformants, we isolated one cDNA (1170 bp), named *FpOAR*
252 (GenBank accession no. AB372882), which was found to encode a deduced 42,873 Da
253 protein. A BLASTp (<http://www.ncbi.nlm.nih.gov/BLAST/>) search revealed that the
254 deduced FpOAR showed 86%, 82%, 73%, 66% and 43% identities with predicted
255 membrane proteins of *Postia placenta* (24) and *Phanerochaete chrysosporium* (23), a major
256 intrinsic protein of *Laccaria bicolor* (22), a hypothetical protein CC1G_06363 of
257 *Coprinopsis cinerea* Okayama 7#130 (4), and a transmembrane protein of *Cryptococcus*
258 *neoformans* var. *neoformans* JEC21 (19), respectively (Fig. 2). These are all basidiomycete

fungi and, in particular, *P. placenta* and *P. chrysosporium* are brown- and white-rot fungi, respectively. However, no biochemical functions have been elucidated for these proteins to date. A close similarity between FpOAR and oxalate-degrading enzymes, such as oxalate decarboxylase (EC 4.1.1.2) and oxalate oxidase (EC 1.2.3.4), was not observed. However, the SOSUI program (<http://bp.nuap.nagoya-u.ac.jp/sosui/>) predicted that FpOAR possesses six transmembrane domains (Supplemental Fig. S1).

Oxalic acid resistance in yeast transformants with the cDNA FpOAR. On plates containing 8.5–10 mM oxalic acid, the yeast transformant possessing the cDNA *FpOAR* (*FpOAR*-transformant) showed clear cell growth, whereas no growth was observed in the control transformant with an empty vector (Figs. 3A, B). At an oxalic acid concentration below 8.5 mM, the growth of the control and *FpOAR*-transformant did not differ significantly (data not shown). In medium with the same pH containing malonate but not oxalate, no difference between the control and *FpOAR*-transformant was observed, showing that oxalate is more toxic than malonate (Fig. 3C). To eliminate the possibility that the *FpOAR*-transformant was resistant to low pH (2.2–1.5), we investigated the growth of the *FpOAR*-transformant on a low-pH plate (Fig. 3D), but no difference in growth between the control and *FpOAR*-transformant was observed at pH 2.2–1.5 and pH 5. We then compared the oxalic acid contents of the *FpOAR*-transformant and the empty vector control grown in the presence of 2 mM oxalic acid. No difference in cell growth was observed between the two cultures at this concentration, but the cellular content of oxalate in the *FpOAR*-transformant strongly decreased to 25% compared with that of the control (Fig. 4).

Oxalate transport in vesicles of the *FpOAR*-transformant. In the presence of

MgATP, membrane vesicles of the *FpOAR*-transformant significantly accumulated [¹⁴C]oxalate, which was 1.4 times greater than that of the control lacking MgATP. When the assay was conducted at 4 °C or with vesicles denatured at 95 °C, oxalate transport did not differ from that of the empty vector control (Fig. 5).

Vanadate and gramicidin D, which are inhibitors of P-type ATPases and a monovalent-selective ionophore that dissipates both the pH gradient and membrane potential, inhibited oxalate transport by 28.5% and 55.8%, respectively (Fig. 6). Valinomycin and NH₄Cl, which abolish $\Delta\Psi$ and ΔpH across the membrane, respectively, inhibited oxalate transport by 34.6% and 34.9%, respectively. In contrast, the inhibitors of ABC transporters, glybenclamide and verapamil, slightly inhibited and did not significantly inhibit, respectively, oxalate transport in *FpOAR*-transformant vesicles. These results are in agreement with the oxalate-transporting activity exhibited by membrane vesicles of *F. palustris* (Fig. 1), and suggest that FpOAR is directly involved in oxalate secretion.

Quantitative real-time PCR analysis of *FpOAR* transcripts in *F. palustris*. The quantity of *FpOAR* transcripts increased concomitantly with accumulation of oxalate in the culture medium (Figs. 7A, B and C). High levels were maintained even in the stationary phase during days 9–13, while oxalic acid accumulation increased (day 13, 34 mM). The amount of *FpOAR* transcripts increased three-fold compared with that of the control when 50 mM oxalic acid was added to the medium (Fig. 8).

DISCUSSION

FpOAR functions as a secondary oxalate transporter conferring oxalic acid resistance in *F. palustris*. In this study, we characterized oxalate transport using membrane vesicles of *F. palustris*. We isolated a cDNA, *FpOAR*, encoding a novel membrane oxalate transporter protein specifically conserved among basidiomycete fungi.

The isolated cDNA *FpOAR* conferred resistance to oxalic acid on the *FpOAR*-transformant (Figs. 3A, B, C and D). The oxalate transport activity in the membrane vesicles of the yeast (Fig. 5) indicated that FpOAR was responsible for oxalate transport. The effects of inhibitors on oxalate transport in membrane vesicles of the *FpOAR*-transformant (Fig. 6) suggest that FpOAR transports oxalate by a secondary transport system, in which ΔpH and $\Delta\Psi$ are the driving force. The effects of the inhibitors on yeast vesicles (Fig. 6) were similar to those on vesicles from *F. palustris* (Fig. 1). Furthermore, expression of *FpOAR* and oxalic acid accumulation in the medium were positively correlated (Fig. 7A, B and C). Expression of *FpOAR* was induced by addition of oxalic acid to the culture (Fig. 8). Collectively, these results strongly suggest the involvement of FpOAR as a secondary oxalate transporter to confer oxalic acid resistance in *F. palustris*.

FpOAR is a plasma membrane-localized novel secondary oxalate transporter. FpOAR is proposed to be a novel oxalate secondary transporter based on three lines of evidence: 1) MgATP was needed for oxalate transport activity; 2) FpOAR does not possess an ATP-hydrolyzing domain (Walker motifs and ABC signature) as in ABC transporters, which function as primary transporters (47); and 3) there is no similarity between FpOAR and known oxalate transporters, e.g. SLC26 family proteins (27), the oxalate:formate

antiport protein, OxIT (21), and the putative yeast monocarboxylate transporter, Mch5 (5).

FpOAR is suggested to be a plasma membrane oxalate efflux transporter based on the lower oxalate content in the *FpOAR*-transformant compared with the control (Fig. 4). The probable cytosolic membrane localization of FpOAR is in agreement with the presence of six putative transmembrane domains in FpOAR (Supplemental Fig. S1). Furthermore, the PSORT program (<http://psort.hgc.jp/>) predicted that FpOAR is localized to the plasma membrane. The fungal plasma membrane H⁺-ATPase generates a proton gradient through the cytosolic membrane (37), which is likely to drive oxalate transport through FpOAR.

FpOAR probably plays a crucial role to maintain carbon metabolism by *F. palustris*. During vegetative growth, *F. palustris* produces oxalate from a glucose carbon source with an 80% theoretical yield based on the amount of carbon in glucose (28). Two intrinsic features of *F. palustris* metabolism facilitate such a high yield of oxalate. First, the precursors of oxalate, glyoxylate and oxaloacetate, are constantly supplied through the GLOX cycle in the peroxisome, in which isocitrate lyase (FPICL1, EC 4.1.3.1) and malate synthase (EC 2.3.3.9) play indispensable roles as key enzymes (28, 29, 35). The FPICL1 and malate synthase of *F. palustris* show high activity even in glucose-grown mycelia (28, 29), which is in sharp contrast to the general GLOX cycle in other microorganisms, in which the functioning of the GLOX cycle is repressed by a glucose carbon source (35). Second, it is proposed that the GLOX cycle of *F. palustris* supplies succinate constitutively to the TCA cycle lacking 2-oxoglutarate dehydrogenase activity (28, 29, 35), by which oxaloacetate can be supplied for cytosolic oxalate production through the TCA cycle as well as the GLOX cycle (28, 29, 35).

Fomitopsis palustris continuously secretes oxalate as the fungus grows. This oxalate secretion is mainly due to continuous production of oxalate in primary carbon metabolism. Furthermore, the acid secretion could be due to the absence of oxalate degradation activity in *F. palustris*, in contrast to oxalate-decomposing white-rot fungi (9, 39, 48, 50) and several brown-rot fungi such as *P. placenta* (25) and *G. trabeum* (10). Moreover, we have suggested that *F. palustris* transports oxalate out of the cells to prevent possible inhibition of intracellular metabolic reactions. For example, oxalate might inhibit the activities of FPICL1 and malate synthase in peroxisomes of *F. palustris* (15, 35), because oxalate competitively inhibits the activities of the two enzymes *in vitro* (30, 31). In addition, oxalate produced from oxaloacetate by cytosolic OAAH in *F. palustris* (1, 35) possibly shows product inhibition for OAAH activity, because oxalate is a competitive inhibitor ($K_i = 19 \mu\text{M}$) for OAAH from *Botrytis cinerea* (13). Therefore, the oxalate production coupled with energy metabolism and the efficient oxalate transport out of the cells are essential to maintain carbon metabolism in *F. palustris*. Aided by the oxalate export system, including FpOAR, and the oxalic acid resistance system, including FpTRP26 (49), carbon metabolism through the TCA and GLOX cycles are probably prevented from inhibition by oxalate *in vivo*. FpTRP26 was predicted to be a soluble protein and might help with oxalate export from the hyphal cells (49). The yeast transformant with FpTRP26 showed similar resistance to oxalic acid with regard to the acid concentration and pH (49). Further research is needed to elucidate how FpTRP26 and FpOAR cooperatively work in the oxalate resistance system. Whether the FpOAR homologous protein functions in oxalate-producing and -degrading brown-rot fungi requires investigation. Furthermore, in the same fungi, a

possible role of oxalate degradation in relation to energy metabolism should be evaluated to clarify the possible role of oxalate metabolism in brown-rot fungi. In this context, a possible ATP-generation by oxalate degradation is hypothesized for *P. placenta* (20) based on gene expression (24) as proposed for white-rot oxalate-degrading fungus *C. subvermispora* in which oxalate degradation by oxalate decarboxylase with formate dehydrogenase could produce NADH to be utilized for ATP synthesis (48).

FpOAR homologous protein is a potential target for development of new wood preservatives. The FpOAR homologous protein may be distributed widely in wood-rotting fungi, because the homologs showing significant identities with FpOAR were found in genomes of the brown- and white-rot fungi *P. placenta* and *P. chrysosporium*, respectively (Fig. 2). Oxalate production and secretion is commonly observed in wood-rotting fungi, although brown-rot fungi accumulate greater amounts of oxalate in the culture fluid than do white-rot fungi (8, 38). Therefore, the FpOAR homologous protein may generally function as an oxalate transporter in wood-rotting fungi. From the viewpoint of wood preservation, if the function of FpOAR is inhibited by wood preservatives, oxalate is expected to be accumulated intracellularly in brown-rot fungi and growth would be seriously damaged. By a similar inhibitory mechanism, oxalate excretion by white-rot fungi would decrease, which may repress lignin degradation, because a certain amount of excreted oxalate is important to stabilize Mn^{3+} oxidation for lignin degradation by manganese peroxidase (18). Accordingly, the FpOAR homologous protein would be a possible target protein to develop a new wood preservative to inactivate oxalate transport for extermination of wood-rotting fungi.

In summary, we have isolated a cDNA, *FpOAR*, encoding a novel oxalate transporter from *F. palustris*. The deduced FpOAR protein is suggested to play an important role in wood decay by acting as a secondary transporter responsible for secretion of oxalate from *F. palustris* hyphal cells. Two strategies for prevention of oxalate toxicity have been found for brown-rot fungi: 1) oxalate efflux through FpOAR; and 2) in addition to oxalate efflux, oxalate degradation in oxalate-producing and -degrading brown-rot fungi. Further characterization of oxalate transport by FpOAR is needed to elucidate the underlying mechanisms. Oxalate transport from the peroxisome to the cytosol remains to be investigated.

REFERENCES

1. **Akamatsu, Y., A. Ohta, M. Takahashi, and M. Shimada.** 1991. Enzymatic formation of oxalate from oxaloacetate with cell-free-extracts of the brown-rot fungus *Tyromyces palustris* in relation to the biodegradation of cellulose. *Mokuzai Gakkaishi* **37**:575-577.
2. **Arantes, V., Y. Qian, A. M. F. Milagres, J. Jellison, and B. Goodell.** 2009. Effect of pH and oxalic acid on the reduction of Fe^{3+} by a biomimetic chelator and on Fe^{3+} desorption/adsorption onto wood: Implications for brown-rot decay. *International Biodeterioration & Biodegradation* **63**:478-483.
3. **Bradford, M. M.** 1976. Rapid and sensitive method for quantitation of microgram quantities of protein utilizing principle of protein-dye binding. *Anal. Biochem.* **72**:248-254.
4. **Broad Institute of MIT and Harvard.** 2003. *Coprinus cinereus* sequencing project (<http://www.broad.mit.edu>).
5. **Cheng, V., H. U. Stotz, K. Hippchen, and A. T. Bakalinsky.** 2007. Genome-wide screen for oxalate-sensitive mutants of *Saccharomyces cerevisiae*. *Appl. Environ. Microbiol.* **73**: 5919-5927.
6. **Decottignies, A., A. M. Grant, J. W. Nichols, H. de Wet, D. B. McIntosh, and A. Goffeau.** 1998. ATPase and multidrug transport activities of the overexpressed yeast ABC protein Yor1p. *J. Biol. Chem.* **273**:12612-12622.
7. **Duchesne, L.C., B. E. Ellis, and R. L. Peterson.** 1989. Disease suppression by the ectomycorrhizal fungus *Paxillus involutus* –contribution of oxalic acid-. *Can. J. Bot.* **67**: 2726-2730.
8. **Dutton, M. V., and C. S. Evans.** 1996. Oxalate production by fungi: Its role in

- 425 pathogenicity and ecology in the soil environment. Can. J. Microbiol.
426 **42**:881-895.
- 427 9. **Escutia, M. R., I. Bowater, A. Edwards, A. R. Bottrill, M. R. Burrnull, R.**
428 **Polanco, R. Vicuña, and S. Bornemann.** 2005. Cloning and Sequencing of two
429 *Ceriporiopsis subvermispora* bicupin oxalate oxidase allelic isoforms:
430 Implications for the reaction specificity of oxalate oxidases and decarboxylases.
431 Appl. Environ. Microbiol. **71**:3608-3616.
- 432 10. **Espejo, E., and E. Agosin.** 1991. Production and degradation of oxalic acid by
433 brown-rot fungi. Appl. Environ. Microbiol. **57**: 1980-1986.
- 434 11. **Gadd, G. M.** 2007. Geomycology: biogeochemical transformations of rocks,
435 minerals, metals and radionuclides by fungi, bioweathering and bioremediation.
436 Mycol. Res. **111**:3-49.
- 437 12. **Green III, F., M. J. Larsen, J. E. Winandy, and T. L. Highley.** 1991. Role of
438 oxalic acid in incipient brown-rot decay. Mater. Org. **26**:191-213.
- 439 13. **Han, Y., H. J. Joosten, W. Niu, Z. Zhao, P. S. Mariano, M. T. McCalman, J.**
440 **A. L. van Kan, P. J. Schaap, and D. Dunaway-mariano.** 2007. Oxaloacetate
441 hydrolase, the C-C bond lyase of oxalate secreting fungi. J. Biol. Chem.
442 **282**:9581-9590.
- 443 14. **Hattori, T., N. Akitsu, G. S. Seo, A. Ohta, and M. Shimada.** 2000. A possible
444 growth promoting effect of the organic acids produced in an axenic symbiotic
445 culture of *Pinus densiflora* and *Lactarius hatsudake* on both of symbionts. Ann.
446 Report. Interdiscipl. Res. Inst. Environ. Sci. **19**:59-65.
- 447 15. **Hattori, T., K. Okawa, M. Fujimura, M. Mizoguchi, T. Watanabe, T.**
448 **Tokimatsu, H. Inui, K. Baba, S. Suzuki, T. Umezawa, and M. Shimada.** 2007

Subcellular localization of the oxalic acid-producing enzyme, cytochrome *c*-dependent glyoxylate dehydrogenase in grown-rot fungus *Fomitopsis palustris*. Cellulose Chemistry and Technol. **41**:545-553.

16. **Hyde, S.M., and P.M. Wood.** 1997. A mechanism for production of hydroxyl radicals by the brown-rot fungus *Coniophora puteana*: Fe(III) reduction by cellobiose dehydrogenase and Fe(II) oxidation at a distance from the hyphae. Microbiology **143**: 259-266.

17. **Klein, M., Y. M. Mammun, T. Eggmann, C. Schüller, H. Wolfger, E. Martinoia, and K. Kuchler.** 2002. The ATP-binding cassette (ABC) transporter Bpt1p mediates vacuolar sequestration of glutathione conjugates in yeast. FEBS Letters **520**:63-67.

18. **Kuan, I. C., and M. Tien.** 1993. Stimulation of Mn-peroxidase activity - A possible role for oxalate in lignin biodegradation. Proc. Natl. Acad. Sci. USA **90**:1242-1246.

19. **Loftus, B.J., E. Fung, P. Roncaglia, D. Rowley, P. Amedeo, D. Bruno, J. Vamathevan, M. Miranda, I. J. Anderson, J. A. Fraser, J. E. Allen, I. E. Bosdet, M. R. Brent, R. Chiu, T. L. Doering, M. J. Donlin, C. A. D'Souza, D. S. Fox, V. Grinberg, J. Fu, M. Fukushima, B. J. Haas, J. C. Cuang, G. Janbon, S. J. M. Jones, H. L. Koo, M. I. Krzywinski, J. K. Kwon-Chung, K. B. Lengeler, R. Maiti, M.A. Marra, R. E. Marra, C. A. Mathewson, T. G. Mitchell, M. Pertea, F. R. Riggs, S. L. Salzberg, J. E. Schein, A. Shgvartsbeyn, H. Shin, M. Shumway, C. A. Specht, B. B. Suh, A. Tenney, T. R. Utterback, B. L. Wickes, J. R. Wortman, N. H. Wye, J. W. Kronstad, J. K. Lodge, J. Heitman, R. W. Davis, C. M. Fraser, R. W. Hyman.** 2005. The

473 genome of the basidiomycetous yeast and human pathogen *Cryptococcus*
474 *neoformans*. Science **307**: 1321-1324.

475 20. **Mäkelä, M.R., K. Hildén, T. K. Lundell.** 2010. Oxalate decarboxylase:
476 biotechnological update and prevalence of the enzyme in filamentous fungi. Appl.
477 Microbiol. Biotechnol. **87**: 801-814.

478 21. **Malony, P.C.** 1994. Bacterial transporters. Current Opinion in Cell Biology
479 **6**:571-582.

480 22. **Martin, F., A. Aerts, D. Ahréen, A. Brun, E. G. J. Danchin, F. Duchaussoy,**
481 **J. Gibon, A. Kohler, E. Lindquist, V. Pereda, A. Salamov, H. J. Shapiro, J.**
482 **Wuyts, D. Blaudez, M. Buée, P. Brokstein, B. Canbäck, D. Cohen, P. E.**
483 **Courty, P. M. Coutinho, C. Delaruelle, J. C. Detter, A. Deveau, S. DiFazio, S.**
484 **Duplessis, L. Fraissinet-Tachet, E. Lucic, P. Frey-Klett, C. Fourrey, I.**
485 **Feussner, G. Gay, J. Grimwood, P. J. Hoegger, P. Jain, S. Kilaru, J. Labbé,**
486 **Y. C. Lin, V. Legué, F. L. Tacon, R. Marmeisse, D. Melayah, B. Montanini,**
487 **M. Muratet, U. Nehls, H. Niculita-Hirzel, M. P. Oudot-Le Secq, M. Peter, H.**
488 **Quesneville, B. Rajashekar, M. Reich, N. Rouhier, J. Schmutz, T. Yin, M.**
489 **Chalot, B. Henrissat, U. Kües, S. Lucas, V. de Peer, G. K. Podila, A. Polle, P.**
490 **J. Pukkila, P. M. Richardson, P. Rouzé, I. R. Sanders, J. E. Stajich, A.**
491 **Tunlid, G. Tuskan, I. V. Grigoriev.** 2008. The genome of *Laccaria bicolor*
492 provides insights into mycorrhizal symbiosis. Nature **452**: 88-92.

493 23. **Martinez, D., L. F. Larrondo, N. Putnam, M. D. Gelpke, K. Huang, J.**
494 **Chapman, K. G. Helfenbein, P. Ramaiya, J. C. Detter, F. Larimer, P. M.**
495 **Coutinho, B. Henrissat, R. Berka, D. Cullen, D. Rokhsar.** 2004. Genome

sequence of the lignocelluloses degrading fungus *Phanerochaete chrysosporium* strain RP78. Nature Biotechnology **22**: 695-700.

24. **Martinez, D., J. Challacombe, I. Morgenstern, D. Hibbett, M. Schmoll, C. P. Kubicek, P. Ferreira, F. J. Ruiz-Duenas, A. T. Martinez, P. Kersten, K. E. Hammel, A. V. Wymelenberg, J. Gaskell, E. Lindquist, G. Sabat, S. S. BonDurant, L. F. Larrondo, P. Canessa, R. Vicuna, J. Yadav, H. Doddapaneni, V. Subramanian, A. G. Pisabarro, J. L. Laví, J. A. Oguiza, E. Master, B. Henrissat, P. M. Coutinho, P. Harris, J. K. Magnuson, S. E. Baker, K. Bruno, W. Kenealy, P. J. Hoegger, U. Kűes, P. Ramaiya, S. Lucas, A. Salamov, H. Shapiro, H. Tu, L. C. Chee, M. Misra, G. Xie, S. Teter, D. Yaver, T. James, M. Mokrejs, M. Pospisek, I. V. Grigoriev, T. Brettin, D. Rokhsar, R. Berka, D. Cullen.** 2009. Genome, transcriptome, and secretome analysis of wood decay fungus *Postia placenta* supports unique mechanisms of lignocelluloses conversion. Proc. Natl. Acad. Sci. USA **106**:1954-1959.
25. **Micales, J. A.** 1995. Oxalate decarboxylase in the brown-rot wood decay fungus *Postia placenta*. Mater. Org. **29**: 177-186.
26. **Micales, J. A.** 1997. Localization and induction of oxalate decarboxylase in the brown-rot wood decay fungus *Postia placenta*. International Biodeterioration & Biodegradation **39**: 125-132.
27. **Mount, D. B., and M. F. Romero.** 2004 The SLC26 gene family of multifunctional anion exchangers. Pflűgers Archive-Eur. J. Physiol. **447**:710-721.
28. **Munir, E., J. J. Yoon, T. Tokimatsu, T. Hattori, and M. Shimada.** 2001 A physiological role for oxalic acid biosynthesis in the wood-rotting basidiomycete *Fomitopsis palustris*. Proc. Natl. Acad. Sci. USA **98**:11126-11130.

- 520 29. **Munir, E., J. J. Yoon, T. Tokimatsu, T. Hattori, and M. Shimada.** 2001. New
521 role for glyoxylate cycle enzymes in wood-rotting basidiomycetes in relation to
522 biosynthesis of oxalic acid. *J. Wood Sci.* **47**:368-373.
- 523 30. **Munir, E., T. Hattori, and M. Shimada.** 2002. Purification and characterization
524 of isocitrate lyase from the wood-destroying basidiomycete *Fomitopsis palustris*
525 grown on glucose. *Arch. Biochem. Biophys.* **399**:225-231.
- 526 31. **Munir, E., T. Hattori, and M. Shimada.** 2002. Purification and characterization
527 of malate synthase from the glucose-grown wood-rotting basidiomycete
528 *Fomitopsis palustris*. *Biosci. Biotechnol. Biochem.* **66**:576-581.
- 529 32. **Nakata, P. A.** 2003. Advances in our understanding of calcium oxalate crystal
530 formation and function in plants. *Plant Sci.* **164**:901-909.
- 531 33. **Otani, M., N. Shitan, K. Sakai, E. M. Martinoia, F. Sato, and K. Yazaki.**
532 2005. Characterization of vacuolar transport of the endogenous alkaloid
533 berberine in *Coptis japonica*. *Plant Physiol.* **138**:1939-1946.
- 534 34. **Page, R. D. M.** 1996. Tree View: An application to display phylogenetic trees on
535 personal computers. *Comput. Appl. Biosci.* **12**:357-358.
- 536 35. **Sakai, S., T. Nishide, E. Munir, K. Baba, H. Inui, Y. Nakano, T. Hattori,**
537 **and M. Shimada.** 2006. Subcellular localization of glyoxylate cycle key
538 enzymes involved in oxalate biosynthesis of wood-destroying basidiomycete
539 *Fomitopsis palustris* grown on glucose. *Microbiology* **152**:1857-1866.
- 540 36. **Schilling, J. S., and J. Jellison.** 2005. Oxalate regulation by two brown rot fungi
541 decaying oxalate-amended and non-amended wood. *Holzforschung* **59**: 681-688.
- 542 37. **Serrano, R.** 1988. Structure and function of proton translocation ATPase in
543 plasma membranes of plants and fungi. *Biochim. Biophys. Acta* **947**:1-28.

- 544 38. **Shimada, M., Y. Akamatsu, T. Tokimatsu, K. Mii, and T. Hattori.** 1997.
545 Possible biochemical roles of oxalic acid as a low molecular weight compound
546 involved in brown-rot and white-rot wood decays. *J. Biotechnol.* **53**:103-113.
- 547 39. **Shimazono, H.** 1955. Oxalic acid decarboxylase, a new enzyme from the
548 mycelium of wood destroying fungi. *J. Biochem.* **42**:321-340.
- 549 40. **Sterling, K. M., P. K. Mandal, B. A. Roggenbeck, S. E. Ahearn, G. A.**
550 **Gerencser, and G. A. Ahearn.** 2007. Heavy metal detoxification in crustacean
551 epithelial lysosomes: role of anions in the compartmentalization process. *The*
552 *Journal of Experimental Biology* **210**:3484-3493.
- 553 41. **Tanaka, N., Y. Akamatsu, T. Hattori, and M. Shimada.** 1994. Effect of oxalic
554 acid on the oxidative break down of cellulose by the Fenton reaction. *Wood Res.*
555 **81**:8-10.
- 556 42. **Thomson, J. D., T. J. Gibson, F. Plewhiak, F. Jeanmougin, and D. G.**
557 **Higgins.** 1997. The CLUSTAL_X windows interface: flexible strategies for
558 multiple sequence alignment aided by quality analysis tools. *Nucleic Acid Res.*
559 **25**:4876-4882.
- 560 43. **Tokimatsu, T., Y. Nagai, T. Hattori, and M. Shimada.** 1998. Purification and
561 characteristics of a novel cytochrome *c* dependent glyoxylate dehydrogenase
562 from a wood-destroying fungus *Tyromyces palustris*. *FEBS Letters*
563 **437**:117-121.
- 564 44. **Tommasini, R., R. Evers, E. E. Vogt, C. Mornet, G. J. R. Zaman, A. H.**
565 **Schinkel, P. Borst, and E. Martinoia.** 1996. The human multidrug
566 resistance-associated protein functionally complements the yeast cadmium
567 resistance factor 1. *Proc. Natl. Acad. Sci. USA* **93**: 6743-6748.

- 568 45. **Varela, E. and M. Tien.** 2003. Effect of pH and oxalate on
569 hydroquinone-derived hydroxyl radical formation during brown rot wood
570 degradation. *Appl. Environ. Microbiol.* **69**: 6025-6031.
- 571 46. **Yamaji, K., H. Ishimoto, N. Usui, and S. Mori.** 2005. Organic acids and
572 water-soluble phenolics produced by *Paxillus* sp 60/92 together show antifungal
573 activity against *Pythium vexans* under acidic culture conditions. *Mycorrhiza*
574 **15**:17-23.
- 575 47. **Walker, J.E., M. Saraste, M. J. Runswick, and N. J. Gay.** 1982. Distantly
576 related sequences in the alpha-subunits and beta-subunits of ATP synthase,
577 myosin, kinases and other ATP-requiring enzymes and a common nucleotide
578 binding fold. *EMBO J.* **1**:945-951.
- 579 48. **Watanabe, T., S. Tengku, T. Hattori, and M. Shimada.** 2005. Purification and
580 characterization of NAD-dependent formate dehydrogenase from the white-rot
581 fungus *Ceriporiopsis subvermispora* and a possible role of the enzyme in oxalate
582 metabolism. *Enzyme Microb. Tech.* **37**:68-75.
- 583 49. **Watanabe, T., N. Shitan, T. Umezawa, K. Yazaki, M. Shimada, and T. Hattori.**
584 2007. Involvement of FpTRP26, a thioredoxin-related protein, in oxalic
585 acid-resistance of the brown-rot fungus *Fomitopsis palustris*. *FEBS Letters*
586 **581**:1788-1792.
- 587 50. **Watanabe, T., T. Fujiwara, T. Umezawa, M. Shimada, and T. Hattori.** 2008.
588 Cloning of a cDNA encoding a NAD-dependent formate dehydrogenase involved
589 in oxalic acid metabolism from the white-rot fungus *Ceriporiopsis*
590 *subvermispora* and its gene expression analysis. *FEMS Microbiol. Lett.*
591 **279**:64-70.

51. **Wipf, D., M. Benjdia, E. Rikirsch, S. Zimmermann, M. Tegeder, and W. B. Frommer.** 2003. An expression cDNA library for suppression cloning in yeast mutants, complementation of a yeast *his4* mutant, and EST analysis from the symbiotic basidiomycete *Hebeloma cylindrosporum*. *Genome* **46**:177-181.

ACKNOWLEDGMENTS

We thank Dr. A. Goffeau (Université Catholique de Louvain, Louvain-la-Neuve, Belgium) for kindly providing the *S. cerevisiae* strain AD12345678, and Dr. W.B. Frommer (Carnegie Institution, Stanford, CA, USA) for the gift of pDR196. This research was partly supported by a Grant-in-Aid for Scientific Research from the Japan Society for the Promotion of Science (No. 19580172), by a grant-in-aid from the Hokuto Foundation for Bioscience, and by a grant-in-aid from Development and Assessment of Sustainable Humanosphere (*DASH*)/Forest Biomass Analytical System (*FBAS*), *Kyoto University (20DF19 and 21DF19)*.

The abbreviations used are: ABC, ATP-binding cassette; FpOAR, Fomitopsis palustris Oxalic Acid Resistance; GLOX, glyoxylate; TCA, tricarboxylic acid

Figure legends

FIG. 1. Oxalate transport and the effect of inhibitors using membrane vesicles from *F. palustris*. Mean value \pm standard deviation.

* $p < 0.05$ ($n = 3$).

FIG. 2. Neighbor-joining tree for FpOAR and its homologs. The tree was generated using ClustalX (42) and visualized with TREEVIEW (34).

AAEY01000042, a transmembrane protein of *Cryptococcus neoformans* var. *neoformans* JEC21 (GenBank accession no. AAEY01000042); gwh2.7.329.1, predicted membrane proteins of *Phanerochaete chrysosporium* (JGI Protein ID 29288; gwh2.7.329.1); Plus.C_740045, predicted membrane proteins of *Postia placenta* (JGI Protein ID 111900; estExt_Genewise1Plus.C_740045); FpOAR (*Fomitopsis palustris* Oxalic Acid Resistance) (GenBank accession no. AB372882); Lbscf0011g04660, a major intrinsic protein of *Laccaria bicolor* (JGI Protein ID 297309; eu2.Lbscf0011g04660); AACS01000187, a hypothetical protein CC1G_06363 of *Coprinopsis cinerea* okayama 7#130 (GenBank accession no. AACS01000187). Numbers at forks are bootstrap values derived from 1000 replicates. The scale bar represents 0.05 substitutions per amino acid position.


FIG. 3. Growth of yeast transformants containing an empty vector (control) and *FpOAR* on SD (–Ura) plates containing (A) no additives (standard), (B) oxalic acid, (C) malonic acid and (D) HCl. Concentration of each additive and pH are shown above each image. The number of yeast cells inoculated on the plate are indicated by  at the top of each figure (A-D).

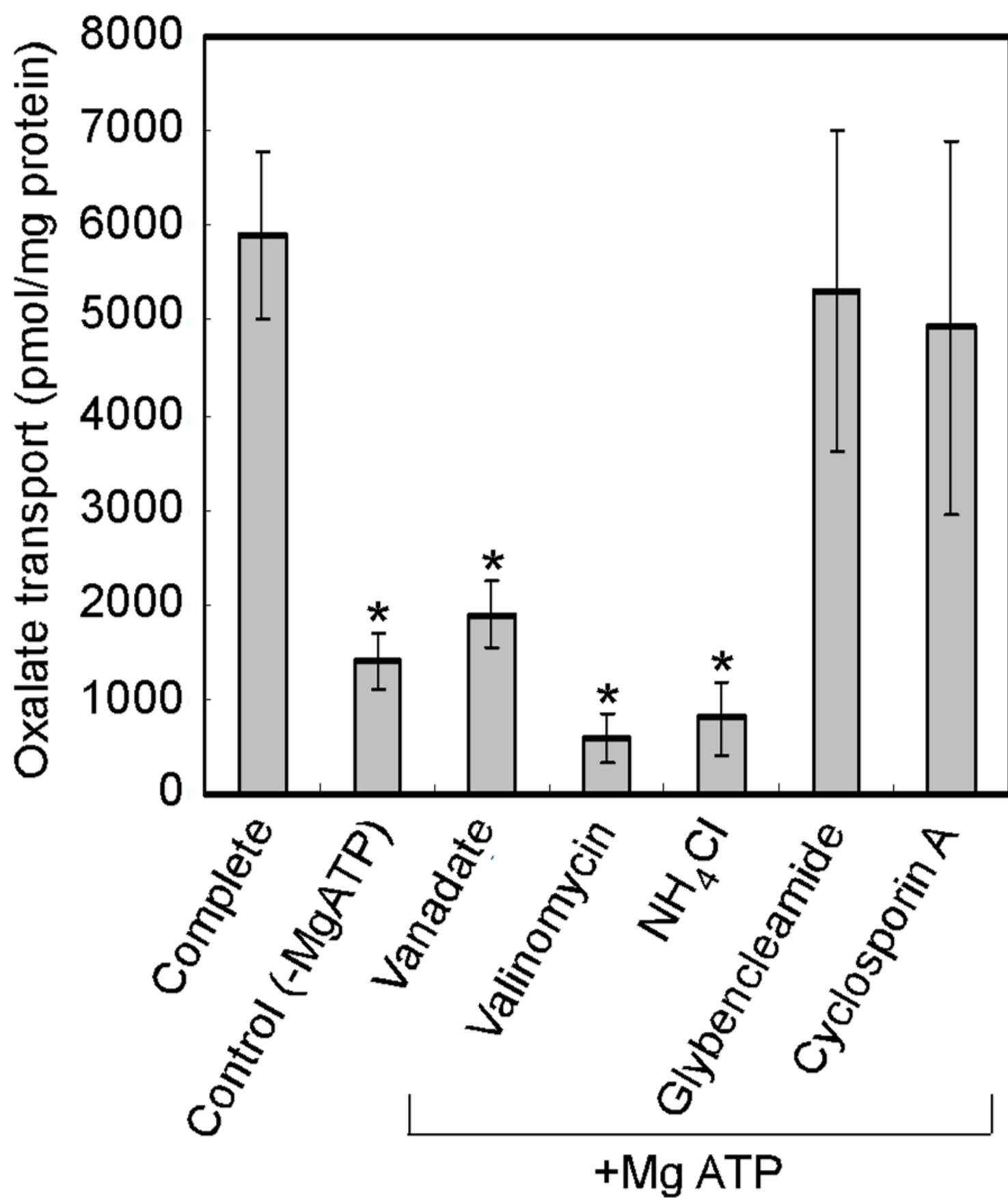
FIG. 4. Amount of oxalic acid in yeast transformants containing an empty vector (control) and *FpOAR*. Mean value \pm standard deviation. ** $p < 0.01$ ($n = 4$).

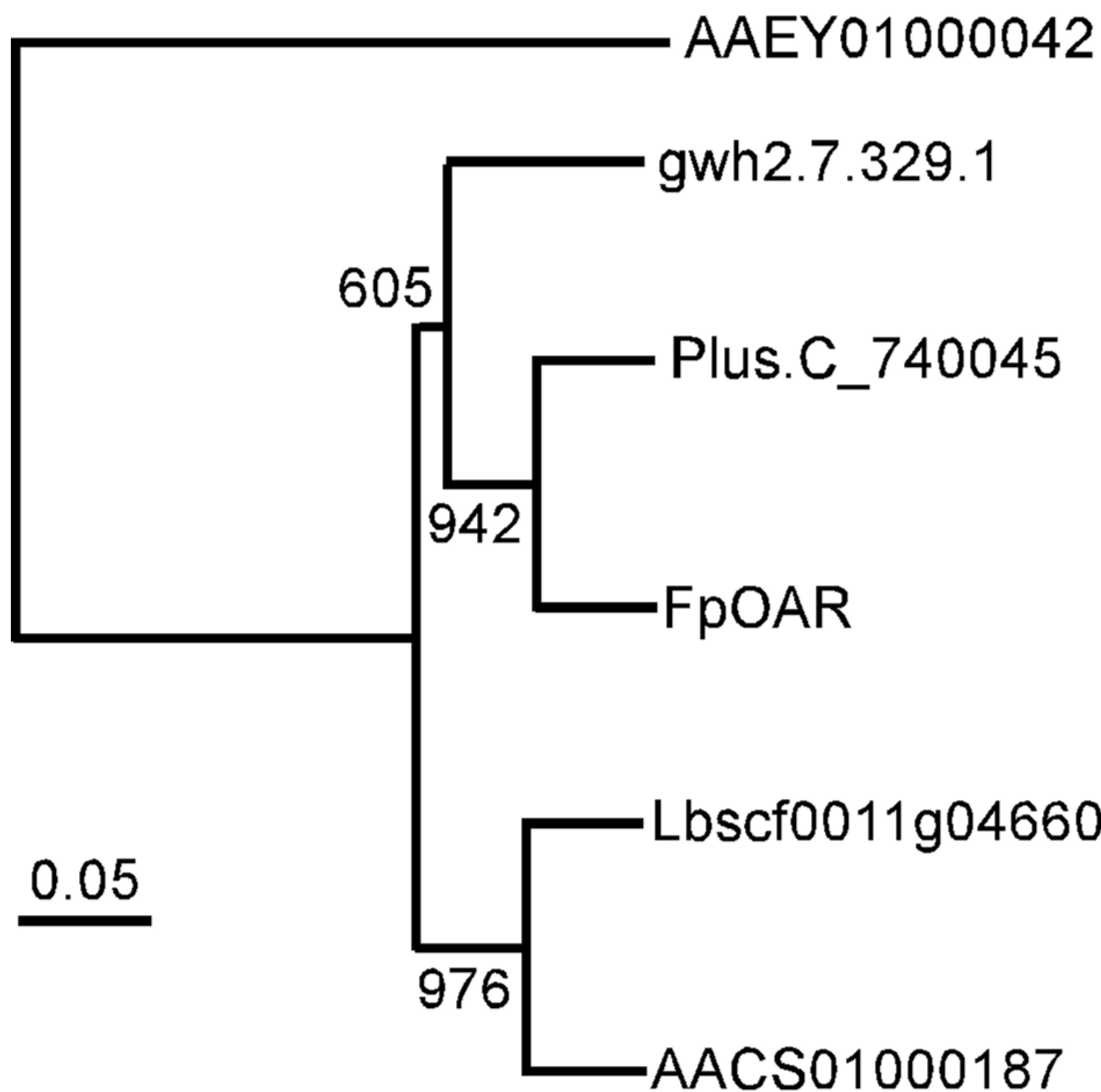
FIG. 5. Oxalate export in yeast transformants containing *FpOAR* (FpOAR-transformant) and an empty vector (control). ** $p < 0.01$ ($n = 4$). The complete system, FpOAR-transformant + MgATP, showed significantly greater oxalate transport with ** than any other system. Denatured: the assay using the vesicles denatured at 95°C; 4°C: the assay conducted at 4°C. Mean value \pm standard deviation.

FIG. 6. Oxalate transport and effect of inhibitors using vesicles prepared from the *FpOAR*-transformant. The reaction was carried out for 20 min. Mean value \pm standard deviation. * $p < 0.05$ ($n = 3$).

FIG. 7. Changes in (A) dry weight of mycelia, (B) oxalic acid accumulated and pH in the medium during culture of *F. palustris*. In (C) the copy number is shown based on 0.2 μ g total RNA, where the copy number is defined as the number of molecules of mRNA coding FpOAR. The mean values and standard deviations were determined based on triplicate samples. Mean value \pm standard deviation.

FIG. 8. Effect of exogenous addition of oxalic acid to the *F. palustris* culture on *FpOAR* transcription. Mean value \pm standard deviation. ** $p < 0.01$ ($n = 4$).





(A) Standard

Cell density 

pH5.0

Control

FpOAR



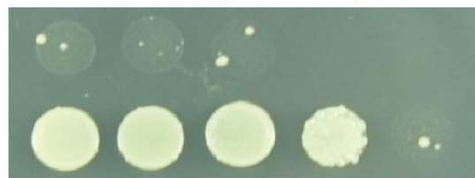
(B) Oxalic acid

Cell density 

8.5 mM (pH 2.5)

Control

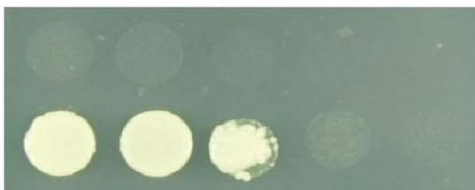
FpOAR



9.5 mM (pH 2.5)

Control

FpOAR



10 mM (pH 2.2)

Control

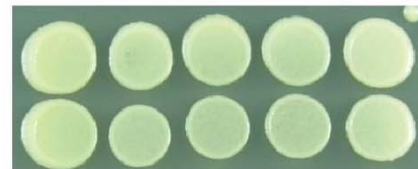
FpOAR



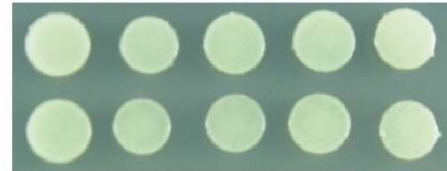
(C) Malonic acid



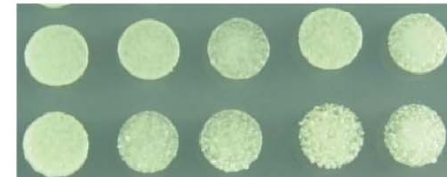
8.5 mM (pH 2.5)



9.5 mM (pH 2.5)



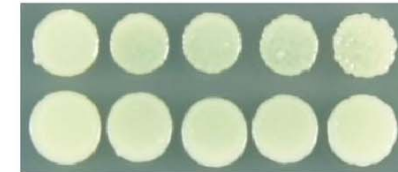
10 mM (pH 2.2)



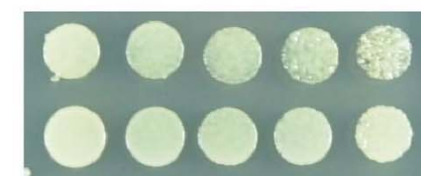
(D) Acidic pH



pH2.2

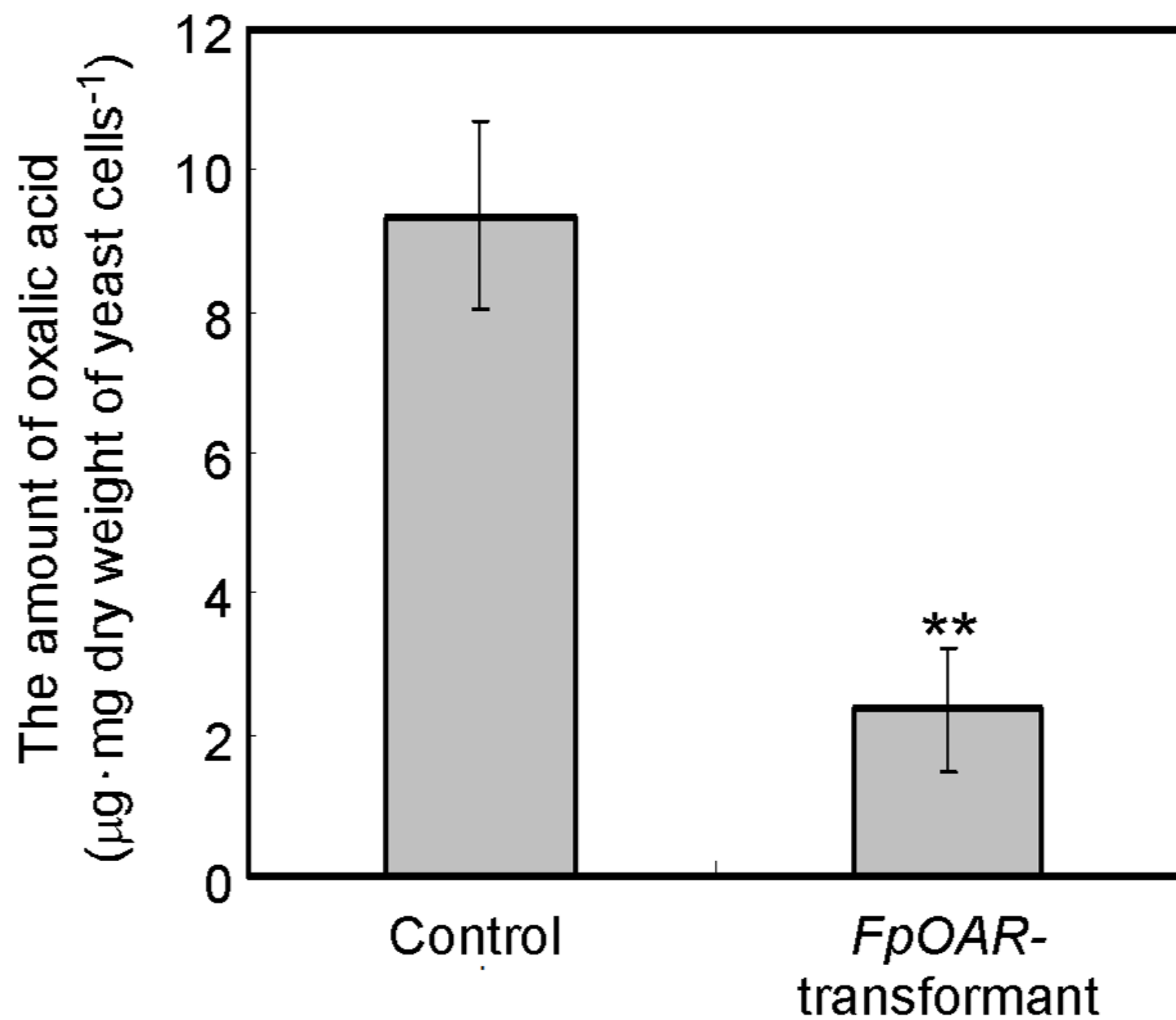


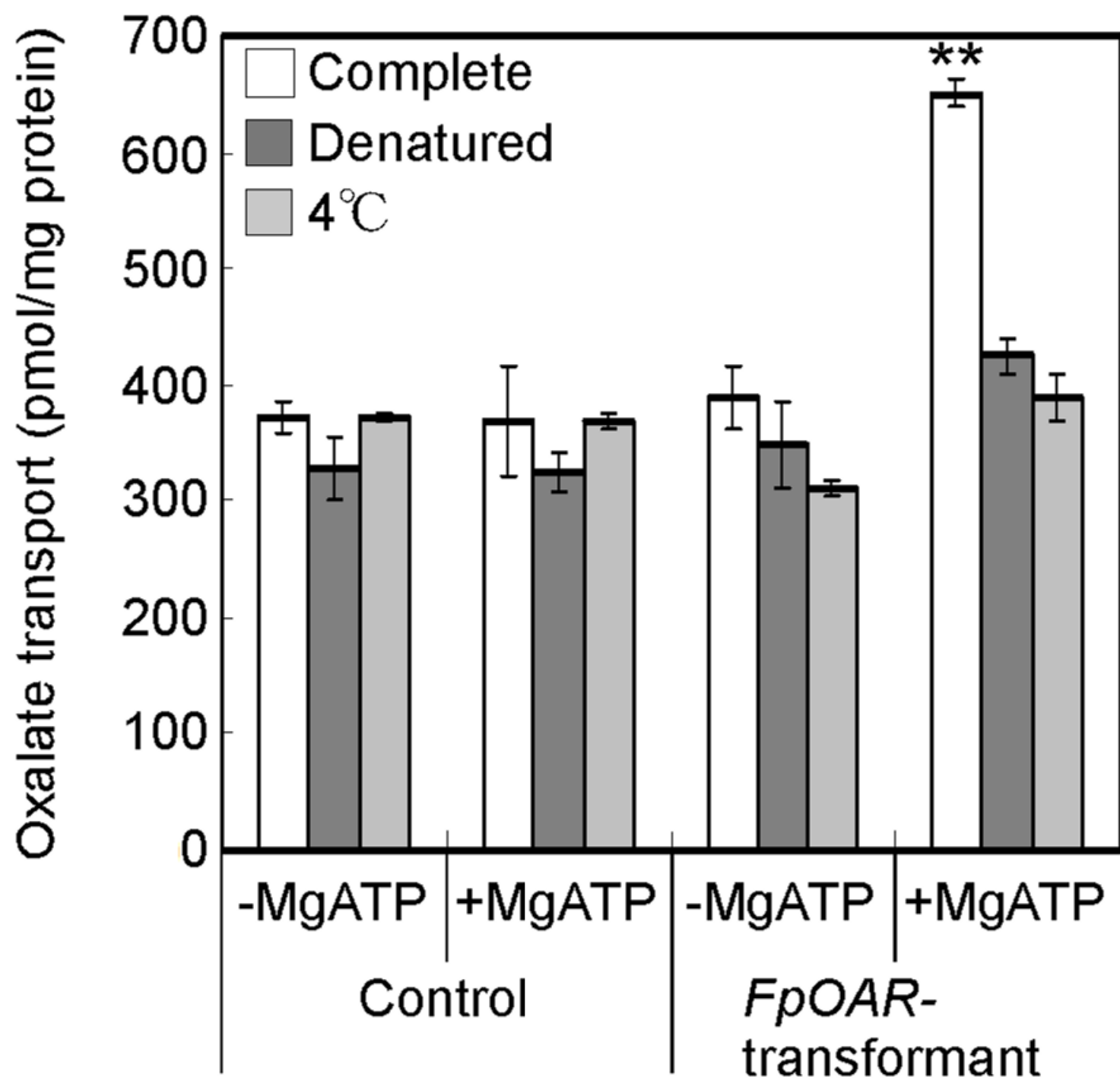
pH1.6

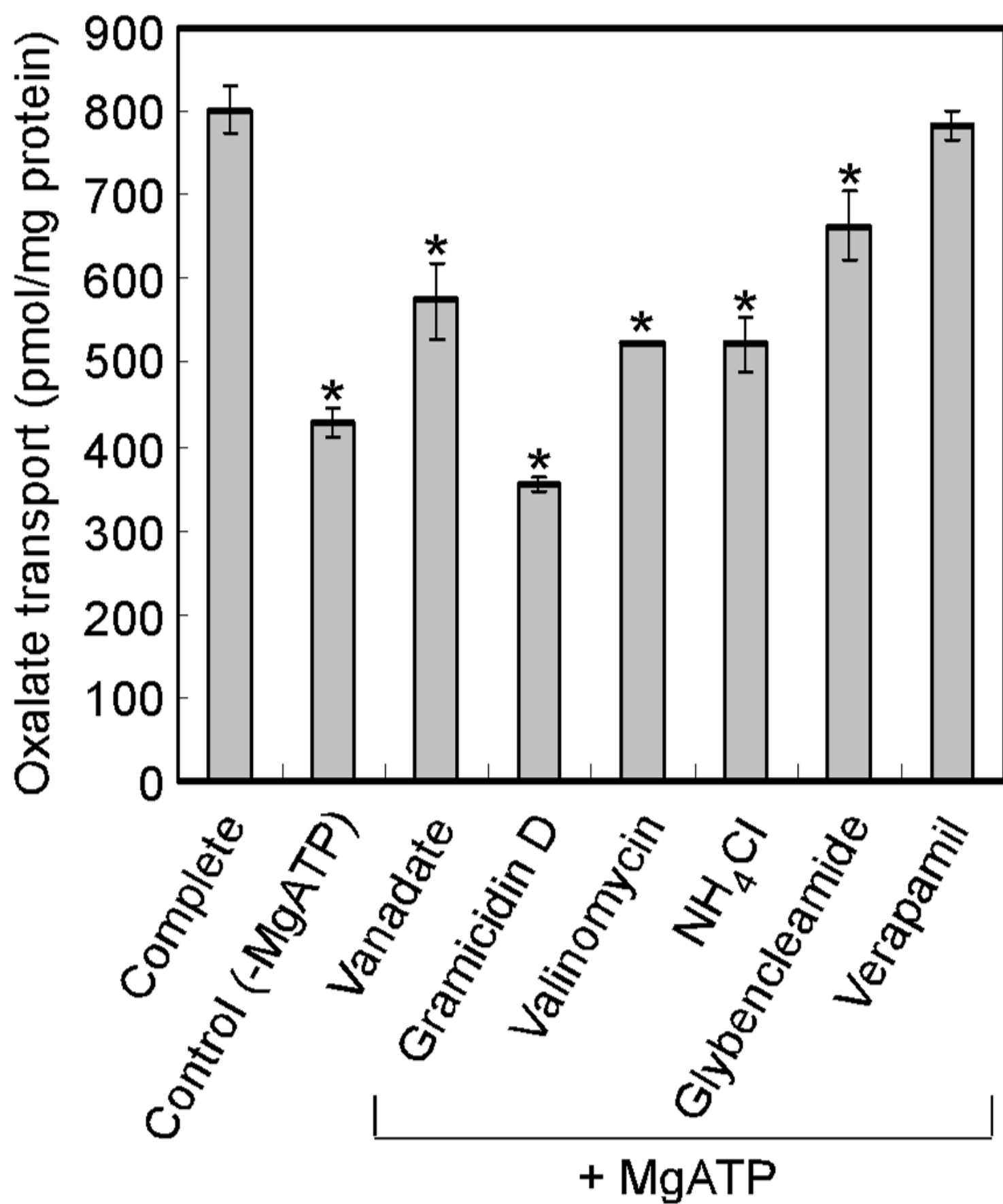


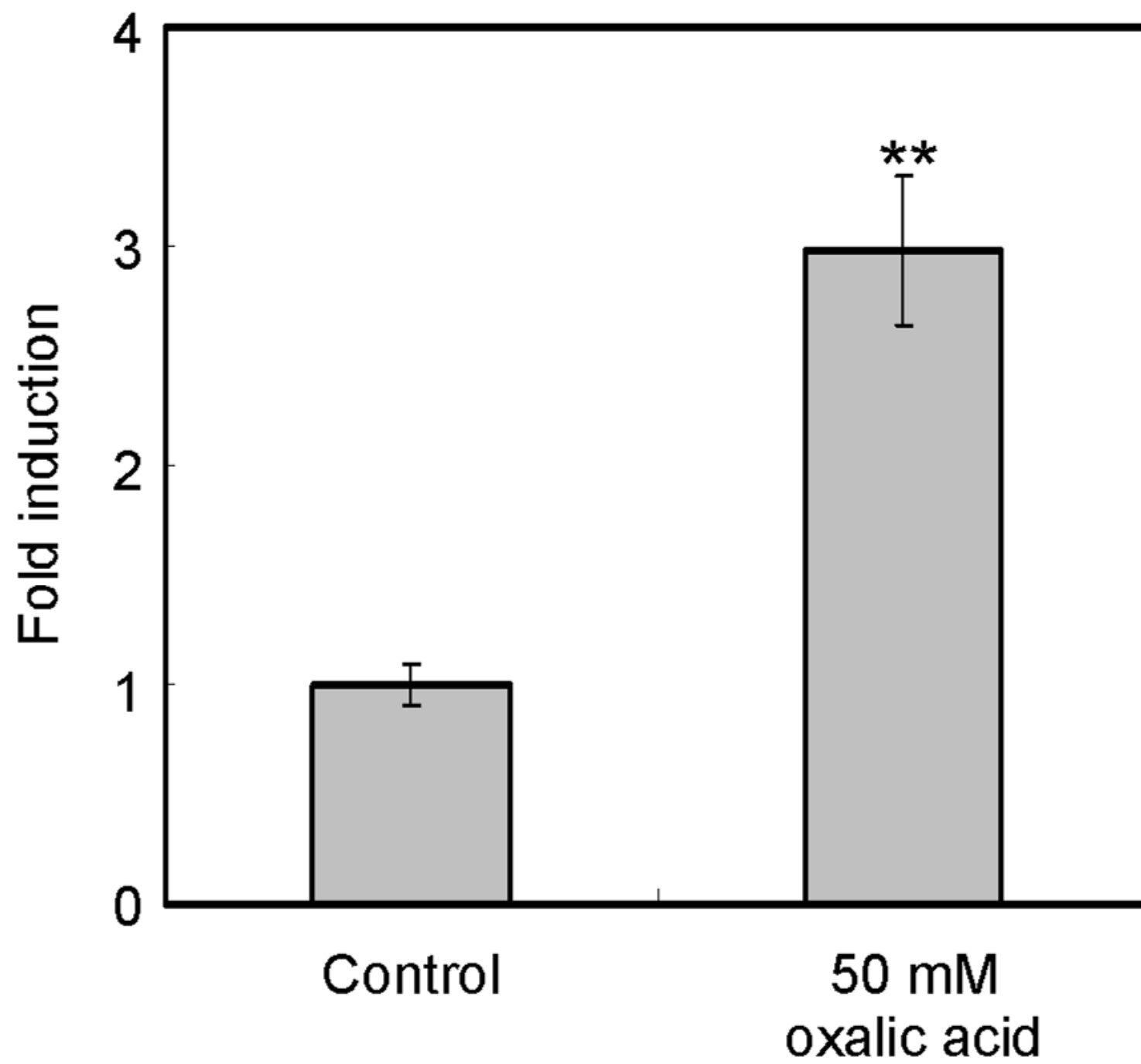
pH1.5

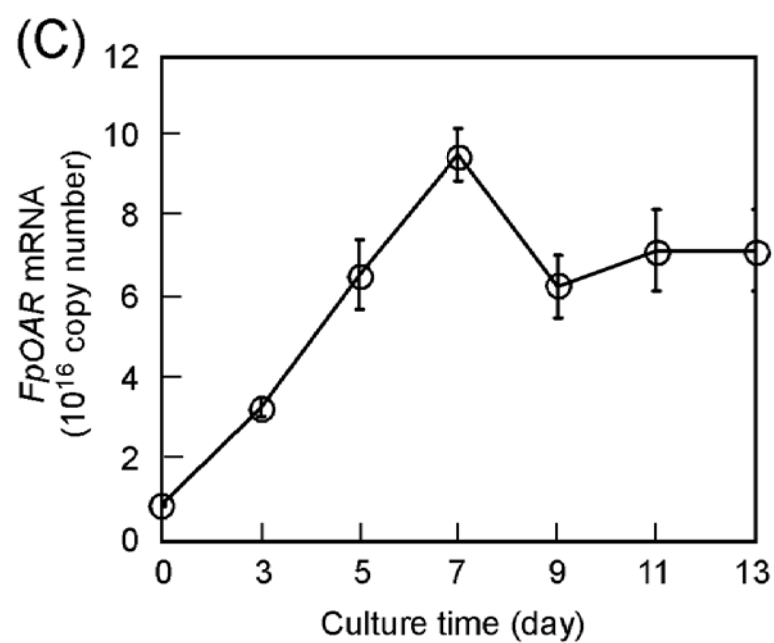
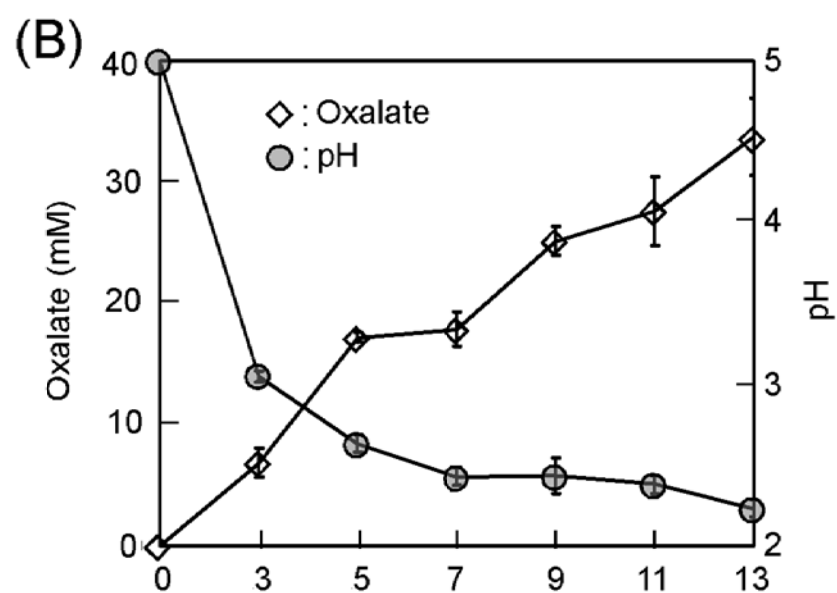
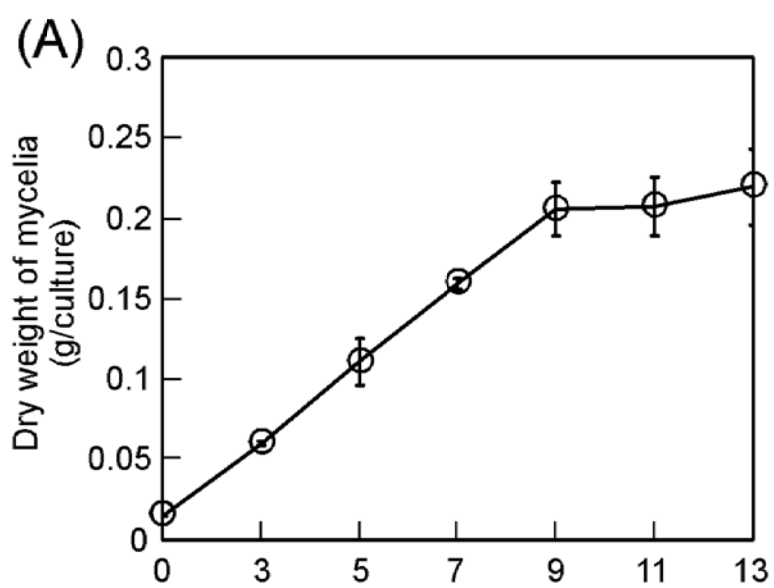












 : Primary helix  : Secondary helix  : Membrane

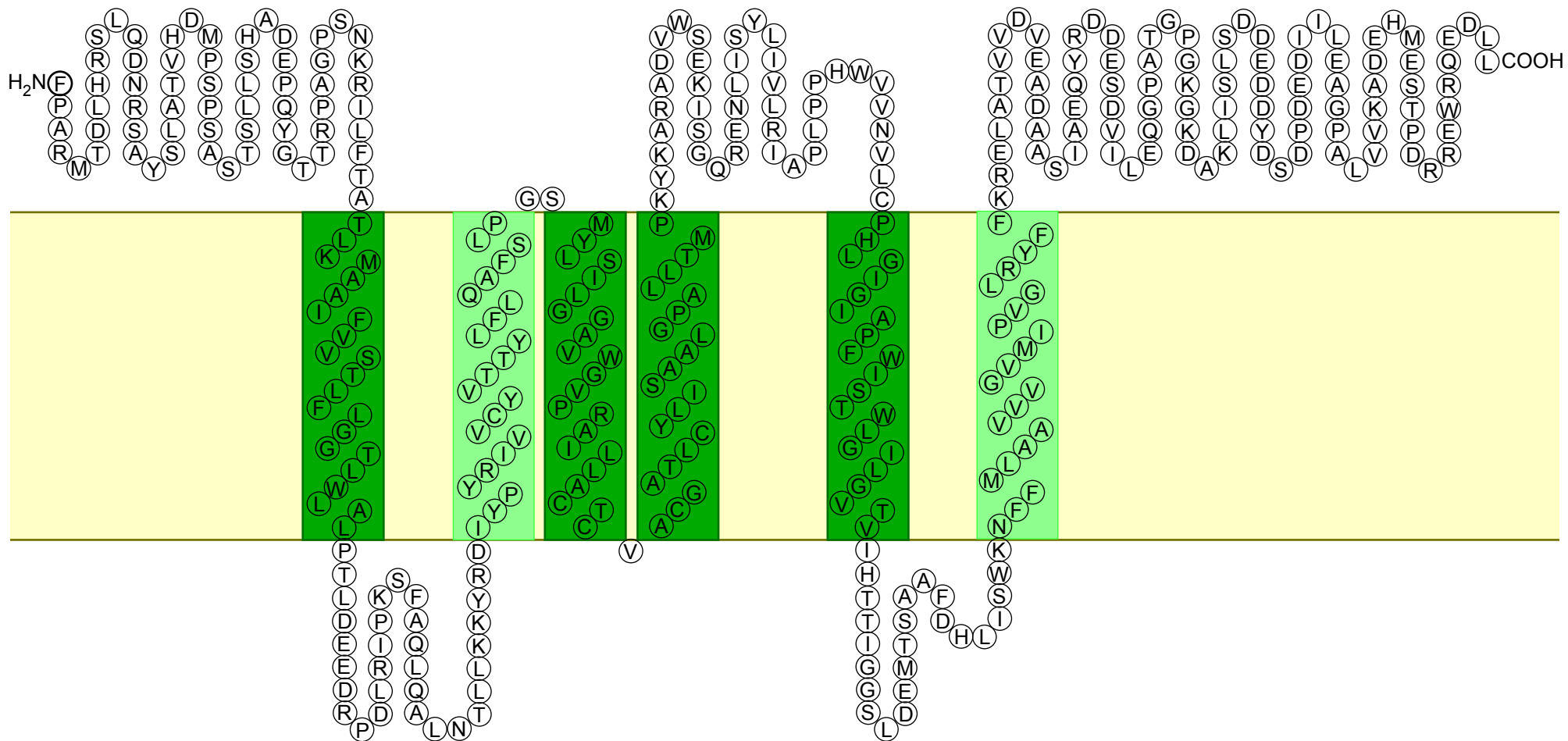


Fig. S1. Predicted transmembrane domains of FpOAR. The prediction was conducted with the SOSUI program (<http://bp.nuap.nagoya-u.ac.jp/sosui/>). The predicted transmembrane domains are shown as primary and secondary helices.